# Adhesion in Polypropylene/Aluminum Laminates Made by Extrusion Coating

**S. Devisme,[1] J.-M. Haudin,[1] J.-F. Agassant,[1] R. Combarieu,[1] D. Rauline,[2] F. Chopinez[2]**

[1]*Centre de Mise en Forme des Matériaux, Ecole des Mines de Paris, UMR CNRS 7635, Sophia Antipolis, France*
[2]*Arkema, Centre de Recherche, Développement, Applications et Techniique de l'Ouest, Serquigny, France*

Received 16 October 2007; accepted 23 July 2008
DOI 10.1002/app.29760
Published online 23 February 2009 in Wiley InterScience (www.interscience.wiley.com).

**ABSTRACT:** The purpose of this article is to study how processing parameters can promote adhesion in grafted polypropylene/aluminum laminates made by extrusion coating. The density of bonds created at the interface is quantified by X-ray spectroscopy after dissolution of the polymer film. dynamic mechanical analysis (DMA) and tensile tests are performed to characterize the mechanical properties of polymer films. They are linked with the crystalline structure, as revealed by optical microscopy and X-ray diffraction. A numerical model of extrusion coating is used to quantify the impact of cooling conditions on adhesion. A good correlation is found between the temperature history, the formation of bonds, and the mechanical properties of the polymer films. High temperature conditions can improve adhesion by increasing the open time for the reaction and the rate of the chemical reaction between grafted polymer chains and aluminum. © 2009 Wiley Periodicals, Inc. J Appl Polym Sci 112: 2609–2624, 2009

**Key words:** adhesion; coatings; crystallization; extrusion; polyolefins

## INTRODUCTION

Multilayered structures, composed of several polymer layers coated on a substrate (e.g., paper, metal foil), are frequently used in packaging industry. A common way to make these structures is extrusion coating. Low density polyethylene is mostly used in such applications, but it tends to be replaced by polypropylene for use at higher temperatures (e.g., sterilization). A good adhesion between the polymer layers and the coated substrate is of prime importance. Adhesion properties of multilayered structures are usually tested using the peel test.[1]

Polypropylenes used in extrusion coating exhibit very low adhesion properties because of their nonpolar character. These properties can be enhanced by numerous methods, such as oxidation, flame treatment, plasma discharge, etc.[2] Another interesting way is to modify adhesion properties by grafting polar groups on the polymer chains. The grafted chain may react with the aluminum surface and chemical bonds are formed with the hydroxyl groups on the "oxidized" metal surface.

In the case of polypropylene, maleic anhydride is commonly used as grafted polar group. Many articles have explored the reaction between maleic grafted polypropylene and aluminum, and the type of bonding has been identified.[3–8] After coating on the aluminum foil, the grafted maleic anhydride molecule is immediately hydrolyzed into maleic acid, as schematically shown in Figure 1. Then, the acid functions form a bridged chelate bond between a carboxylate group and two aluminum cations at the oxide surface. High temperatures enhance this chemical reaction.[6] The chemical reaction has been investigated mainly for specimens prepared by compression molding.[4,7,9,10] In these conditions, the open time for the reaction (5–30 min at 180–220°C) is much longer than in extrusion coating (<1–2 s). Conversely, few reports deal with the temperature history during extrusion coating,[11,12] (i.e., the space and time temperature variations), and more specifically with its impact on the chemical reaction at the interface and the adhesion properties.[13]

The aim of the present work is to show how process conditions can promote adhesion in grafted polypropylene–aluminum laminates made by extrusion coating. It first highlights the different experiments carried out to characterize the structure and the mechanical properties of polymer films, to examine the interface before and after peeling, and to quantify the surface density of grafted chains linked with aluminum oxide. It then illustrates the impact of processing conditions on structure and morphology, as revealed by microscopic observations of thin microtomed film sections and X-ray diffraction experiments. A thermomechanical model presented

*Correspondence to:* J.-M. Haudin (jean-marc.haudin@ensmp.fr).

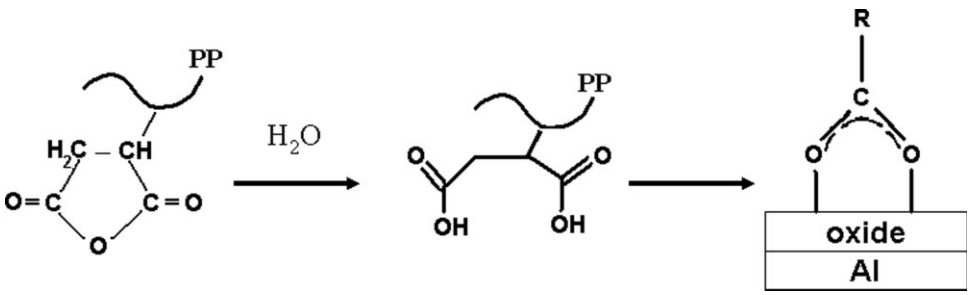


**Figure 1** Chemical reaction between maleic anhydride grafted onto the polymer chains and the aluminum oxide. Schematic representation from Refs. 6 and 8.

elsewhere[14] is used to calculate the temperature history, especially close to the interface, and to predict the crystallization location. Finally, adhesion properties are discussed in terms of mechanical anchoring into the porous surface, surface density of bonds, and mechanical properties of polymer films, and correlated to processing conditions.

## MATERIALS AND EXPERIMENTAL METHODS

### Materials

The multilayered structures made by extrusion coating consisted of the three different layers indicated in Figure 2: a random copolymer layer (polypropylene–ethylene) named CoP, a grafted polypropylene layer named GPP (Arkema), and an aluminum foil (37 μm). GPP was functionalized with maleic anhydride.

Experiments were carried on the Arkema experimental extrusion coating line described in Figure 3, which manufactures multilayered films (up to three layers) coated onto an aluminum foil. An extruded polymer film is coated on a substrate in a rolling mill consisting of a chill roll and a flexible pressure roll, and then cooled along the process line. This versatile set-up allows us to easily vary processing parameters and to perform temperature measurements at different locations (noted $T_1$ to $T_6$ in Fig. 3), but by construction (dimensions of the machine), extrusion velocity and line speed are smaller than in industrial coating conditions. The thickness of the die-slit opening was 0.3 mm and the die width was 250 mm. The main process parameters are the extrusion temperature ($T_{ext} \approx$ [280°C–300°C]), the extrusion velocity ($U_0$), the stretching distance ($X$ = 6 cm), the line speed ($U_t$), the temperature of the successive chill rolls ($T_{CR1}$, $T_{CR2}$, $T_{CR3}$), and of the nip roll ($T_{NR}$). Extrusion velocity, line speed, and temperature of the chill rolls were tested to know their impact on adhesion properties. Moreover, we used several times an insulating layer of polystyrene (80 μm) to reduce the cooling effect of the chill roll. This additional layer was extruded at the same time as the polypropylene/grafted polypropylene layer (Runs 7–10). In these cases, the multilayered structure obtained after coating on the aluminum foil was PS/CoP/GPP/Al. All the processing conditions considered in this article are listed in Table I.

### Characterization of the multilayered structure

#### Characterization of the film structure

The different crystalline phases and the average degree of crystallinity of extruded structures were determined by X-ray diffraction. The diffraction patterns were recorded using a Panalytical Expert-Pro equipment (Panalytical S.A.S., Limeil-Brévannes, France) monochromatic Cu $K\alpha_1$ radiation. For crystallinity measurements, intensity versus 2θ was collected in the reflection mode by using a Bragg-Brentano mounting.

In addition, thin sections in the thickness of the films were observed by microscopy to investigate the morphology. These thin sections [thickness = 2.5 μm, width = 80 μm (thickness of the film), length = 5 mm] were cut out with a cryogenic ultra-

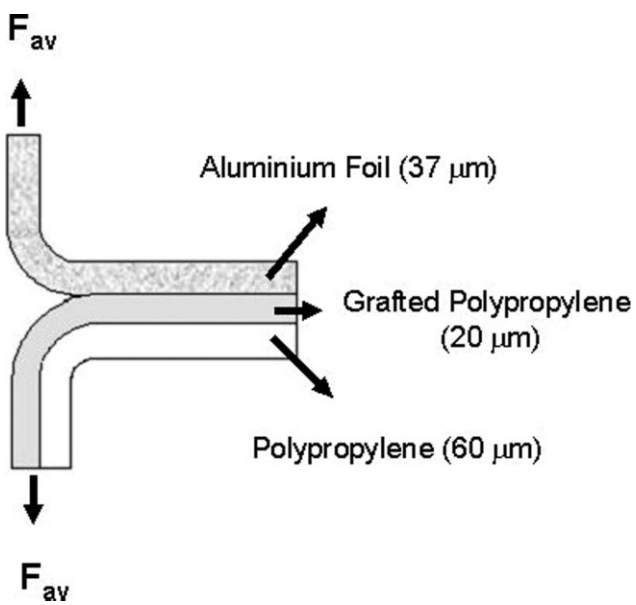


**Figure 2** Sample dimensions for the T-peel test. Description of the different layers.

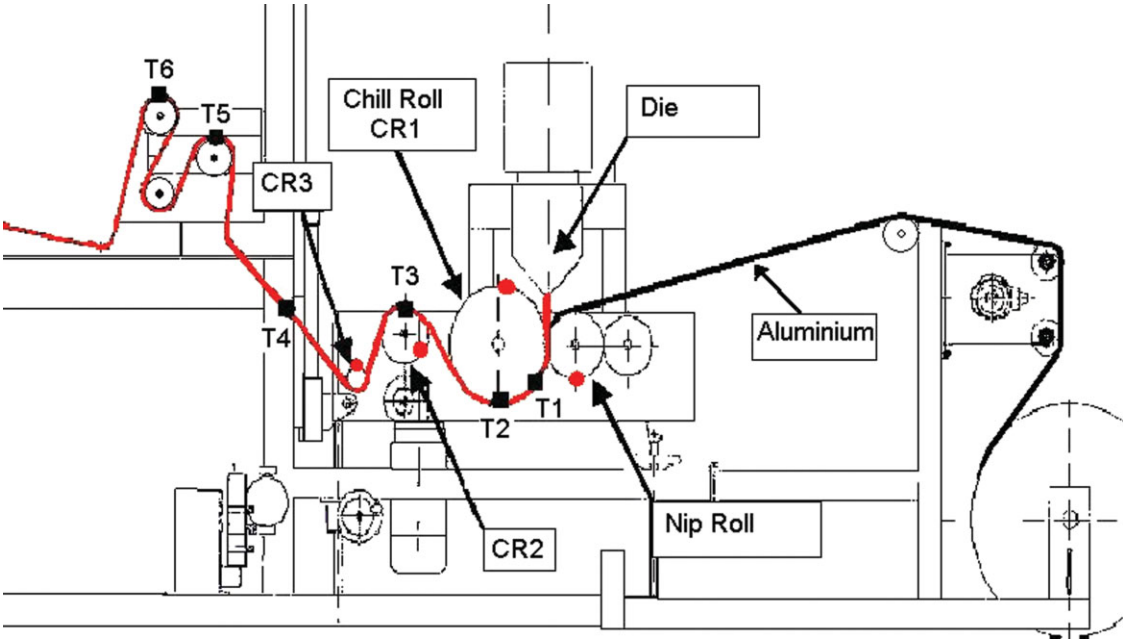


**Figure 3** Description of the extrusion coating line and localization of temperature test points: chill roll temperatures (●), surface temperatures of the multilayered structure (■). [Color figure can be viewed in the online issue, which is available at www.interscience.wiley.com.]

microtome and put between two glass slides with a liquid of refractive index close to the average index of the polymer. The morphology was observed with a gypsum plate between crossed polarizers using a transmission optical microscope (Leica DMRX, Leica Microskopie und Systeme GmbH, Wetzlar, Germany).

### Adhesion measurements and mechanical characterization

The adhesive strength between grafted polypropylene layer and aluminum foil was measured using a T-peel test. The sample dimensions are given in Figure 2. They were adjusted to obtain an angle of 180° between the two strips (aluminum foil and polymer film) during the peel test. Peeling test at room temperature (25°C) was performed with an Erichsen Testwell tensile tester equipped with a 10 N load cell, at a cross-head speed of 200 mm/min. Peel energy $G_p$ is given by:

$$G_p = \frac{2F_{av}}{b} \quad (1)$$

where $F_{av}$ is the applied force and $b$ the width of the test piece (15 mm). For each process conditions, the adhesive strength was measured five times for

**TABLE I**
**Process Operating Data and Corresponding Values of the Peel Force $F_{av}$**

| Runs | Additional layer | $T_{melt}$ (2 cm) | $T_{NR}$ | $T_{CR1}$ | $T_{CR2}$ | $T_{CR3}$ | $U_0$ (m/s) | $U_t$ (m/s) | Draw ratio Dr = $(U_t/U_0)$ | Mean elongation rate ($s^{-1}$) | $F_{av}$ (N) |
|---|---|---|---|---|---|---|---|---|---|---|---|
| 1 | | 282 | 94 | 56 | 20 | 24 | 0.101 | 0.416 | 4.1 | 5.3 | 1.0 |
| 2 | | 282 | 88 | 70 | 26 | 34 | 0.162 | 0.667 | 4.1 | 8.4 | 1.1 |
| 3 | | 266 | 61 | 23 | 14 | 16 | 0.020 | 0.083 | 4.1 | 1.1 | 0 |
| 4 | | 267 | 77 | 92 | 16 | 17 | 0.020 | 0.083 | 4.1 | 1.1 | 0 |
| 5 | | 281 | 97 | 100 | 25 | 56 | 0.101 | 0.416 | 4.1 | 5.3 | 1.4 |
| 6 | | 294 | 90 | 105 | 21 | 80 | 0.162 | 0.667 | 4.1 | 8.4 | 2.2 |
| 7 | Polystyrene | 295 | 104 | 94 | 22 | 68 | 0.101 | 0.416 | 4.1 | 5.3 | 8.2 |
| 8 | Polystyrene | 291 | 103 | 75 | 15 | 30 | 0.020 | 0.083 | 4.1 | 1.1 | 0.8 |
| 9 | Polystyrene | 292 | 110 | 103 | 18 | 37 | 0.020 | 0.083 | 4.1 | 1.1 | 3.2 |
| 10 | Polystyrene | 292 | 111 | 120 | 22 | 88 | 0.101 | 0.416 | 4.1 | 5.3 | – |
| 11 | | 232 | 48 | 16 | 14 | 14 | 0.020 | 0.083 | 4.1 | 1.1 | 0 |
| 12 | | 256 | 86 | 51 | 18 | 22 | 0.101 | 0.416 | 4.1 | 5.3 | 0.9 |
| 13 | | 232 | 69 | 91 | 15 | 17 | 0.020 | 0.083 | 4.1 | 1.1 | 0 |
| 14 | | 257 | 87 | 99 | 21 | 65 | 0.101 | 0.416 | 4.1 | 5.3 | 1.1 |

$T_{melt}$ is measured at 2 cm from the die exit. The mean elongation rate is defined as $(U_t - U_0)/X$.

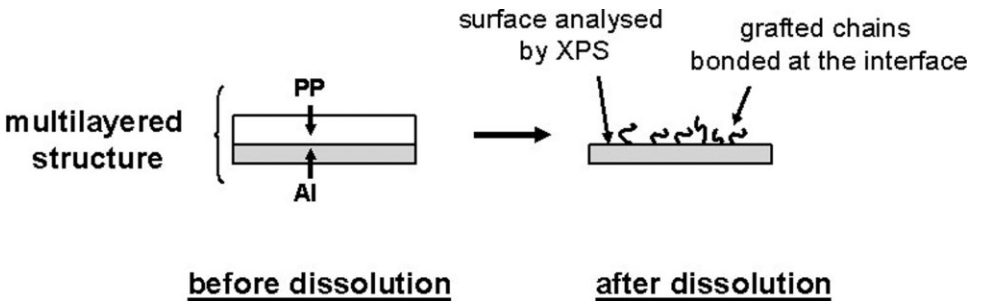


**Figure 4** Scheme of the sample for the XPS analysis before and after dissolution: classical procedure to quantify the density of bonds.

reproducibility. The mean peel force $F_{av}$ was then considered (standard deviation $< 0.1$ N).

The film mechanical properties (Young's modulus and yield stress) were also determined for several process conditions. We used a DMA apparatus (Tritec 2000, Bohlin Instruments, France, Sophia, Antipolis, France) to measure the elasticity modulus. These measurements were achieved by applying a small displacement (10 μm) on thin rectangular strips (5 mm × 5 mm × 80 μm) during 5 min at one frequency (1 Hz) and at room temperature (25°C). The average elasticity modulus was calculated from five DMA tensile tests. In addition, tensile tests were performed with an Erichsen Testwell tensile tester (Testwell, Saint Germain en Laye, France) to obtain the yield stress of each film. Experiments were run at room temperature with a constant cross-head velocity of 3.3 mm/s and a 200 N load cell. The Videotraction® (Apollor Union, Moncell-Lès-Lunéville, France) system was used to measure strain during the tensile test. This method allows us to measure strain by following the displacement of several points drawn on the sample surface with a video camera. Hourglass-shaped samples were machined out with a specific press knife. Only two points were used to determine strain.

### Characterization of the interface

Surface roughness of both grafted polypropylene and aluminum foil was analyzed by atomic force microscopy (AFM) and noncontacting surface microtopography to characterize the wetting of the aluminum foil by the polymer. The grafted polypropylene interface was obtained by dissolution of the aluminum foil in a hydrochloric acid bath during 5 min. The aluminum interface was obtained by dissolution of the polymer layer in a xylene bath at 100°C during 20 min. Surface microtopography was analyzed with an Altisurf 500 apparatus (Altimel, Thonon-les-Bains, France). A computer software (Altimap) allowed us to obtain 3D-pictures of surface and roughness parameters. The analyzed surface dimensions were around 2 × 2 mm$^2$. AFM (Digital Instruments/VEECO, Plainview, NY) with a noncontact mode probe was used to analyze surface characteristics at a much smaller scale (15 × 15 μm$^2$).

### Characterization of the interface by XPS

The polymer/aluminum interface was analyzed by X-ray Photoelectron Spectroscopy to estimate the density of grafted polymer chains which had reacted with aluminum oxides. To estimate it, one of the two materials had to be removed. As shown in Figure 4, we chose to dissolve the polymer film in a xylene bath and to evaluate quantitatively the remaining amount of grafted chains on the aluminum surface. Therefore, polymer film was dissolved in hot xylene at 100°C during a fixed time, which was determined after a specific investigation detailed further (see "Impact of the dissolution conditions"). We tested several dissolution times in the range of 10-60 min to know the impact of time on the surface density values. Aluminum foil was successively rinsed in ethanol and heptane before analysis.

#### X-ray photoelectron spectroscopy

Spectra were collected on a Riber apparatus (Mac 2 system, Riber, Bezons, France) using an Al K$\alpha_1$ source ($h\nu = 1486.6$ eV). The dimensions of the analyzed surface were around 3 × 3 mm$^2$. Survey scans between 0

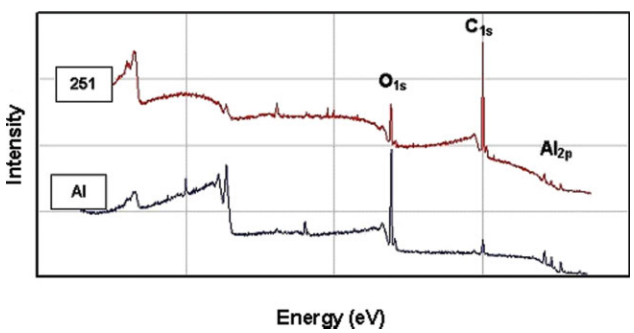


**Figure 5** Typical XPS spectrum of a multilayered structure (labeled 251) after dissolution of the polymer film and comparison with that of a pure aluminum foil (labeled Al). [Color figure can be viewed in the online issue, which is available at www.interscience.wiley.com.]

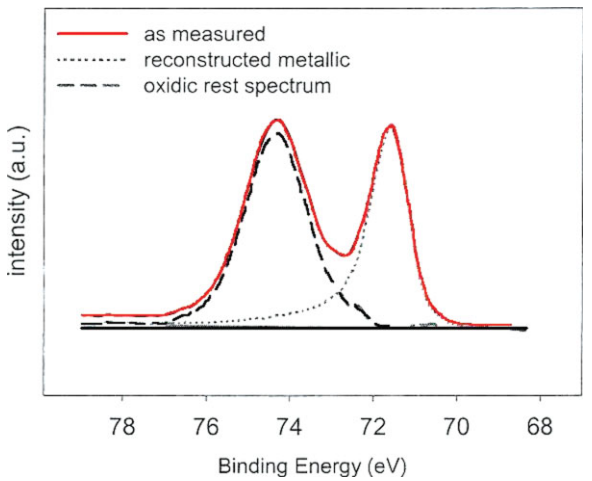


**Figure 6** $Al_{2p}$ spectrum: decomposition of the aluminum peak into a metallic and an oxide component. [Color figure can be viewed in the online issue, which is available at www.interscience.wiley.com.]

and 1400 eV (step 1 eV) were acquired to identify each component of the analyzed surface. A typical spectrum of a multilayered structure after dissolution is displayed in Figure 5 and compared with the one of a pure aluminum foil. Only peaks of C, O, and Al were observed on these scans. Then, window spectra were collected (step 0.1 eV) for $Al_{2p}$, $C_{1s}$, $O_{1s}$ near 71.5, 285, and 530 eV, respectively. All these spectra were taken at an average take-off angle of 90° between the sample and the detector. The intensity of each peak was calculated by integrating the scan after a Shirley background subtraction. Moreover, $Al_{2p}$ peaks were split into two parts (74 eV and 71.5 eV) and fitted using Gaussian peak shapes to know the oxide layer contribution, as indicated in Figure 6.

### Density of grafted chains linked to the aluminum oxides

Figure 7 shows a model of the aluminum surface system after dissolution. It consists of a metallic layer covered by an oxide and a carbon layer of thickness $d_{ox}$ and $d_C$, respectively. It is assumed that the surfaces are flat and that the carbon layer is homogenous in thickness and only composed of grafted chains which are linked with the aluminum oxides. These assumptions allow us to calculate the surface density of bonds at the interface. This density Σ can be related to the carbon layer thickness $d_C$ through eq. (2)[15]:

$$\Sigma = \frac{N_a \rho}{M_n} \cdot d_c \qquad (2)$$

where $N_a$ is Avogadro's number, ρ is the density of GPP, and $M_n$ the number-average molar weight of GPP.

The estimate of each layer thickness ($d_c$ and $d_{ox}$) is based on an iterative method proposed by van den Brand.[16] The experimental intensity ratios $I_{Al2p,met}/I_{C1s}$, $I_{Al2p,ox}/I_{O1s,ox}$, and $I_{Al2p,met}/I_{O1s,ox}$ are compared with the theoretical ones to calculate $d_c$ and $d_{ox}$ by minimizing the deviation between calculated and experimental values. For each condition, the $d_c$ value was measured two or three times for reproducibility. The mean density Σ was then calculated (standard deviation for $\Sigma < 0.003$ ch/nm$^2$).

## RESULTS AND DISCUSSION

### Evaluation of the surface density of bonds

#### Impact of the dissolution conditions

We investigated the impact of two dissolution parameters (time and temperature) to choose the best conditions of dissolution. Two different samples were tested (Runs 3 and 7). They were obtained in two extreme process conditions, given in Table I, and corresponded to poor and high adhesive strengths, respectively. First, Figure 8(A,B) shows that the carbon layer thickness measured by XPS decreases abruptly in the first times of dissolution (<10 min) for both samples and then remains stable after 15 min. This indicates that grafted or nongrafted polymer chains which are not linked with aluminum oxides are totally removed after 15 min. Only polymer chains bonded at the interface constitute the carbon layer characterized by XPS. On the other hand, Figure 9(A) indicates that the temperature of dissolution has no impact on results above 90–100°C. At lower temperature, the polymer layer is only partially removed out from the aluminum surface, even for long dissolution time. We chose the following dissolution conditions to evaluate the surface density of bonds for each process conditions:

- First, the polymer layers are dissolved in a xylene bath at 100°C for 10 min and rinsed in ethanol for 5 min.
- Then, a second dissolution is made for 15 min, to remove the last polymer chains which are not linked with the aluminum oxides.

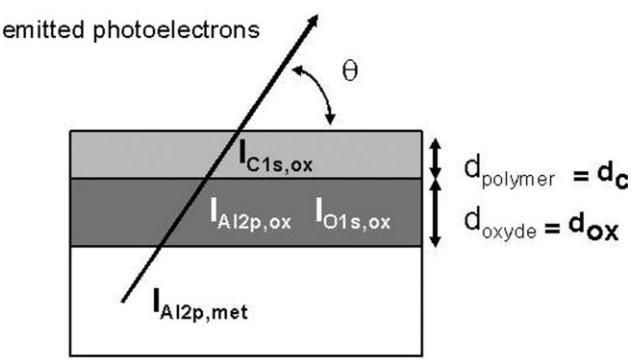


**Figure 7** Schematic representation of the system analyzed by XPS.

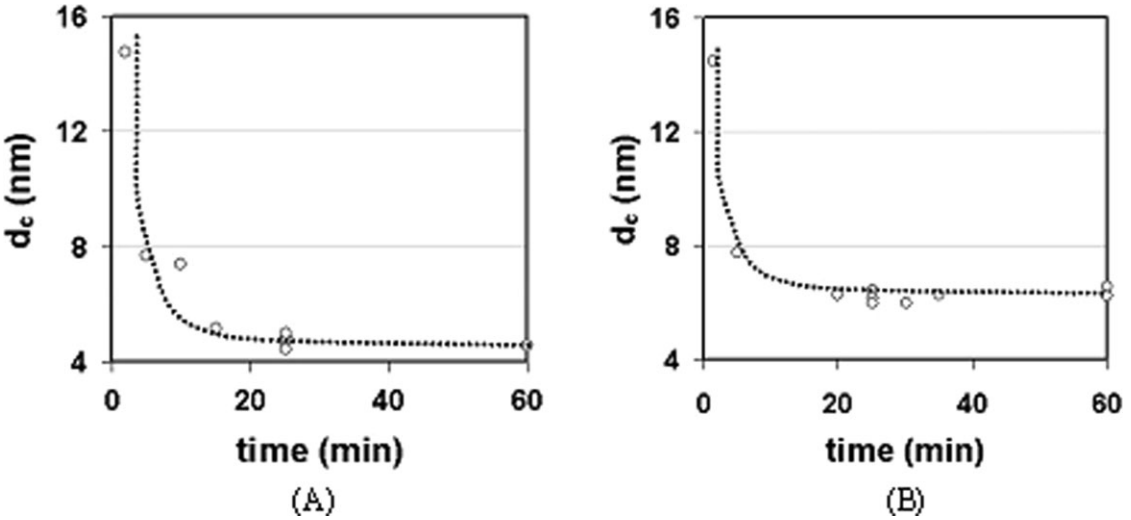


**Figure 8** Decrease of the carbon layer thickness $d_c$ as a function of dissolution time: (A) case of poor adhesive strength (Run 3) and (B) case of high adhesive strength (Run 7).

- Finally, the aluminum foil is rinsed successively in solvents before analysis.

We also applied this protocol to measure the carbon layer present on a native aluminum foil, on which no polymer layer has been deposited by extrusion coating. Figure 9(B) compares the results for native aluminum, Runs 4 and 7, and reveals that the amount of carbon of extruded samples is significantly higher. Moreover, the greater the carbon layer thickness, the higher the peel strength [$F_p$(Run 4) = 0 N, $F_p$ (Run 7) = 8.2 N]. The origin of the carbon layer fixed onto the native aluminum foil is well known. An aluminum surface shows its maximum bonding capacity just after a surface treatment. When this surface is exposed to ambient air for a long period, water is absorbed on the oxide surface and several air-born organic or inorganic contaminants can be also absorbed. It results in a decrease of the bonding capacity of the surface.[17–19] Despite this layer absorbed on the surface, the grafted polypropylene can react with the remaining free oxide sites. As a conclusion, this increase in the amount of absorbed carbon after extrusion coating can be clearly attributed to the grafted polymer chains which are linked with the aluminum oxides.

### Additional reaction between grafted polymer and aluminum during dissolution

During dissolution, an additional reaction can occur between aluminum oxide and the free grafted polymer chains, which are already dissolved in the

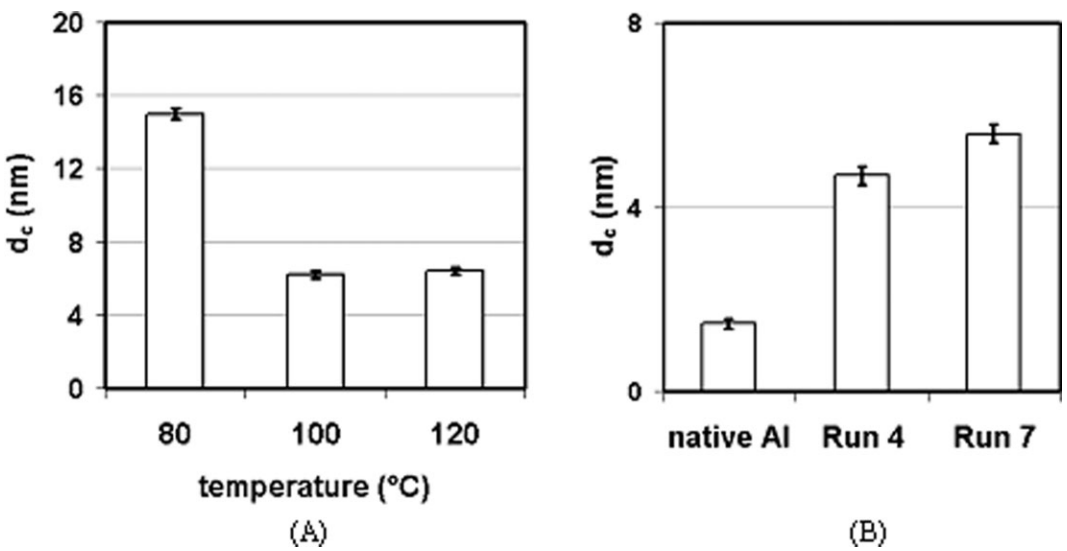


**Figure 9** (A) Influence of dissolution temperature on XPS measurements. (B) Comparison between the carbon layer thicknesses of extruded samples and native aluminum foil measured after dissolution in hot xylene.

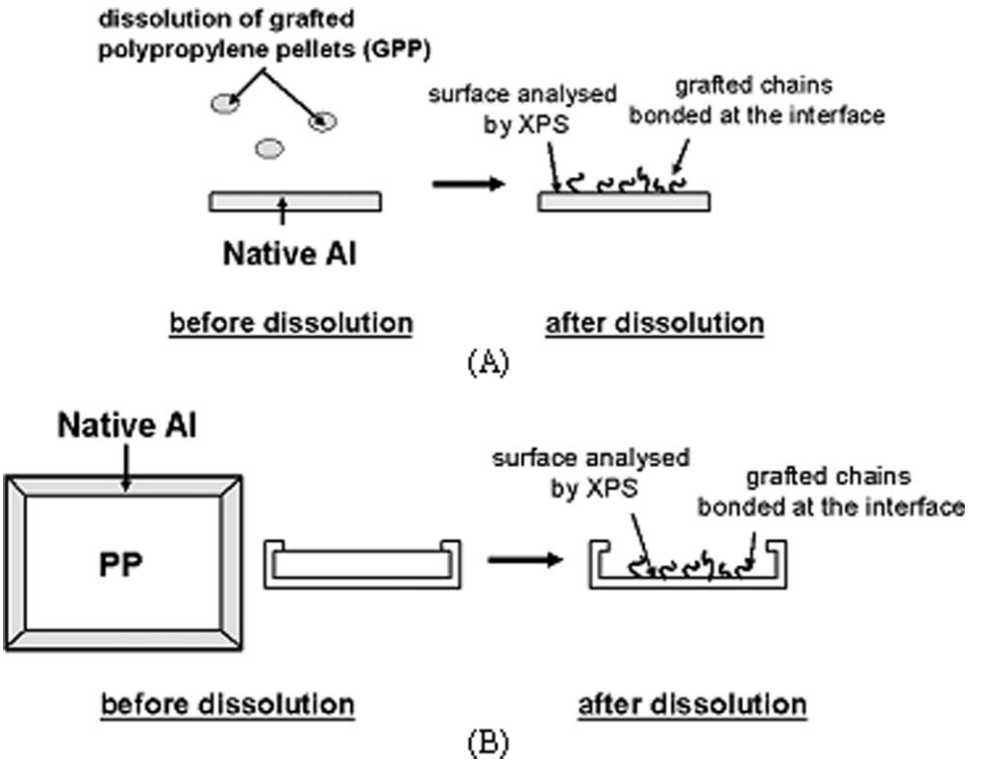


**Figure 10** Scheme of the sample for the XPS analysis before and after dissolution: (A) sample preparation to quantify the reaction between the free grafted chains in solution and aluminum oxide (Experiment A); (B) specific preparation of the samples to evaluate the additional reaction during the time necessary for xylene to diffuse from the polymer surface to the interface (Experiment B).

xylene bath. This reaction can be significant, especially if the free polymer chains are close to the interface. Two experiments were carried out to understand and quantify this additional reaction. They are described in Figure 10. First, we applied the dissolution protocol to a native aluminum foil (xylene, 100°C, 25 min) and increased the grafted polymer concentration $C_{GPP}$ in the xylene bath from 0 to 1.9 g/L [Experiment A described in Fig. 10(A)]. The specific concentration "0.06 g/L" which corresponds to the grafted polypropylene concentration existing in a sample analyzed by XPS (size 10 × 10 $mm^2$) has been chosen as a reference. The plot of $d_c$ versus grafted polypropylene concentration $C_{GPP}$ shows in Figure 11 that the amount of carbon absorbed to aluminum oxides increases slowly with the concentration of free grafted polypropylene chains existing in the xylene bath. Even at high concentration (1.9 g/L), the thickness of the absorbed carbon layer is twice as small as that of the carbon layer absorbed in the case of Run 4, whose adhesion is very poor. These results clearly demonstrate that the amount of grafted chains absorbed to the aluminum surface during extrusion coating is more important than during dissolution.

However, this experiment only shows that the free grafted chains react slowly in solution when the carbon layer is totally removed from the aluminum surface. The additional reaction might be more important during the dissolution time. Indeed, the polymer layer is not removed instantaneously when

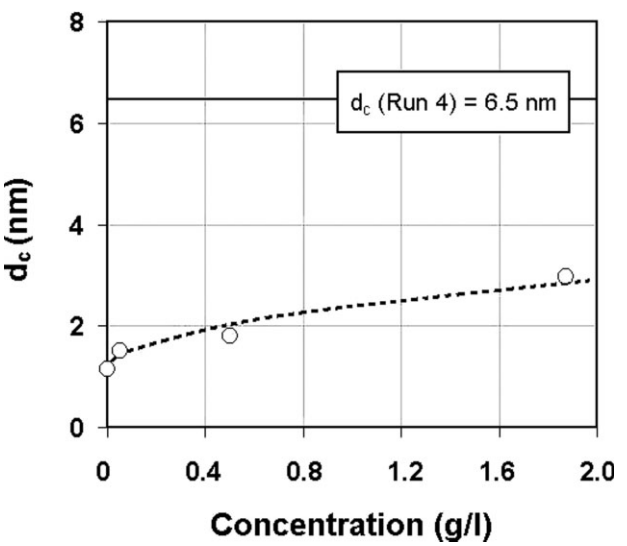


**Figure 11** Additional reaction during dissolution: increase of the carbon layer thickness $d_c$ as a function of the concentration of the free grafted polymer chains in the xylene bath.

the multilayered structure is plunged into the hot xylene bath, as an induction time is necessary for xylene to diffuse from the polymer surface to the interface. As the grafted polymer chains remain close to the interface during the diffusion time, they may react quickly with aluminum oxide. To check this hypothesis, we applied the dissolution protocol to a specific sample [Experiment B in Fig. 10(B)], which consists of a polymer multilayered film deposited on a native aluminum foil. To prevent unsticking during dissolution, the aluminum foil was mechanically maintained against the surface of the polymer film. Figure 12 presents the data issued from Experiments A and B, the carbon thickness originally present on the native aluminum foil and the $d_c$ extremums for extruded structures. A close comparison between these results points out that the additional reaction is more significant when the grafted chains are close to the interface. Indeed, the chemical reaction kinetics of free grafted polymer chains in solution is clearly lower (Experiment A), because a grafted chain have to be close to the interface to react. However, the carbon layer thicknesses remain smaller than the measured thicknesses in the case of extruded structures.

Finally, it is interesting to note that this additional reaction will depend on the bonding capacity of the aluminum surface, which is clearly a function of the density of the grafted chains already bonded at the interface. The experimental differences in $d_c$ values observed between Figure 8(A,B) will be minimized in reality. Indeed, the initial density of bonded polypropylene molecules increases the steric hindrance and leads to a lowering of the additional reaction rate. Then, the higher the initial density of bonds, the smaller the amount of additional bonded chains during dissolution.

Although the additional reaction tends to move all the results closer, we have found this XPS analysis protocol to be a reliable technique to determine Σ. This value seems to give realistic information about the amount of links created at the interface.

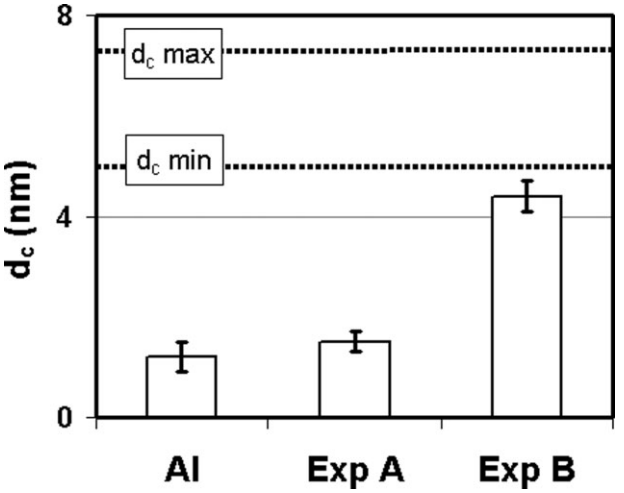


**Figure 12** Comparison between the results for native aluminum, Experiments A and B and $d_c$ extremums measured on extruded structures after dissolution.

## Structure of the films

### X-ray measurements

Each structure was investigated by wide-angle X-ray diffraction. This method provides information about the type of crystalline phase and the degree of crystallinity ($X_c$). Figure 13(A–E) shows the X-ray patterns for several characteristic process conditions. The degrees of crystallinity calculated with Weidinger and Hermans' method[20] are given in Table II.

Different crystalline phases can be identified in polypropylene according to the cooling conditions.[21] The most common is the α phase, characterized by four main diffraction peaks visible in Figure 13(B,C). In several cases (temperatures above 100°C), β phase can appear. This phase is revealed by the presence of an additional peak at 16°, which can be seen in Figure 13(D). Polypropylene also crystallizes in a mesomorphic (or smectic) phase under fast cooling rates or at low temperature.[21] This unstable phase can be observed on Figure 13(A) which displays two broad diffraction peaks at 15° and 21°.

We also observed on X-ray patterns a mixture of different phases due to complex cooling conditions. Figure 13(E) points out, for example, the presence of three phases (amorphous, smectic, and a small amount of α phase). To distinguish their contribution to the overall signal, partial contributions of each phase were separated by fitting the experimental data with a weighted combination of single peaks (amorphous, alpha, and smectic phases).

These structures are representative of those obtained in all process conditions. Nevertheless, X-ray analysis does not allow us to discriminate the structures of the grafted polypropylene and of the random copolymer layers.

### Microscopy

The morphology in the thickness is very heterogeneous for each process condition, because of the dissymmetrical cooling of the multilayered structure. This is revealed by microscopic observations of thin sections in Figure 14. Three major zones can be distinguished in the CoP-layer:

- A transcrystalline morphology is observed at the surface directly in contact with the roll or with the additional polystyrene layer. The occurrence of transcrystallinity can be attributed to an important heterogeneous nucleation at the roll or

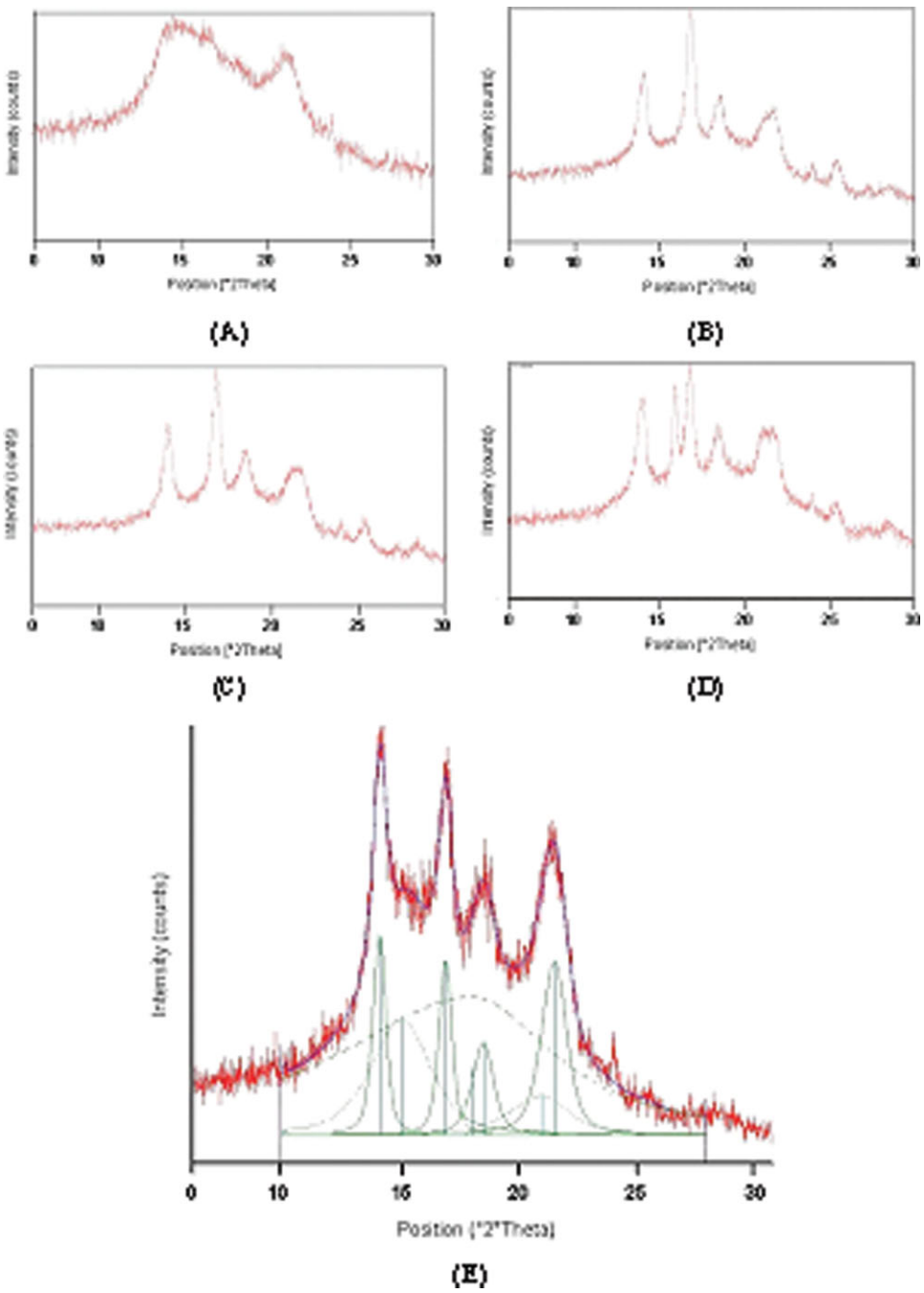


**Figure 13** X-ray patterns of the polypropylene films for different process conditions: (A) Run 3: $U_t = 0.08$ m/s and $T_{CR1} = 23°C$, (B) Run 4: $U_t = 0.08$ m/s and $T_{CR1} = 92°C$, (C) Run 8: $U_t = 0.08$ m/s and $T_{CR1} = 75°C$, (D) Run 9: $U_t = 0.08$ m/s and $T_{CR1} = 103°C$, and (E) Run 7: $U_t = 0.42$ m/s and $T_{CR1} = 94°C$. [Color figure can be viewed in the online issue, which is available at www.interscience.wiley.com.]

polystyrene surface. The thickness of this transcrystalline region increases with the temperature of the roll, as already reported.[22]

- Then, the CoP-layer presents a spherulitic morphology, the size of the spherulites, and the crystalline phase (α, α-β) depending on cooling conditions. Smectic phase can sometimes be observed for critical cooling rates (Run 3).
- At the interface between the copolymer CoP-layer and the GPP layer, another transcrystalline zone can grow during cooling, particularly in the case of high temperature conditions (Runs 4, 8, and 9).

Because of the small thickness of the GPP layer, the observation by optical microscopy cannot allow us to describe the specific crystalline structure of

**TABLE II**
**Crystalline Phases, Degree of Crystallinity ($X_c$), and Mechanical Properties of Films**

| Runs | Yield stress $\sigma_y$ (MPa) ± 0.5 | Young's modulus $E$ (GPa) ± 0.03 | Crystalline phases | $X_c$ (%) ± 3 |
|---|---|---|---|---|
| 1 | 28 | 0.7 | α | 30 |
| 2 | 28 | 0.7 | α | 30 |
| 3 | 22.5 | 0.55 | smectic | 5 |
| 4 | 32.5 | – | α | 37 |
| 5 | 26.5 | 0.65 | smectic + α | 23 |
| 6 | 32 | – | α | 41 |
| 7 | 26.5 | 0.68 | smectic + α | 21 |
| 8 | – | – | α | 36 |
| 9 | 30 | 0.95 | α + β | 36 |
| 10 | – | – | α | 40 |

this layer for all the runs. This could be achieved by transmission electron microscopy, but the preparation of the samples is difficult.

## Interpretation

The general model developed in Ref. 14 was used to predict the temperature history, i.e., the variations of temperature with space and time, and especially the polymer crystallization location. As the process is stationary, we calculate in fact the temperature field. We have plotted on Figure 15(A,B) the surface temperatures of the multilayered structure along the cooling line. Figure 15(A) points out the different cooling steps with the boundary conditions (contact with a roll or with air) and Figure 15(B) shows the good agreement between predicted and experimental surface temperatures along the whole process and for several process conditions.

The model allows us to explain the X-ray patterns and the microscopy observations. For instance, β phase was revealed only for Run 9 when

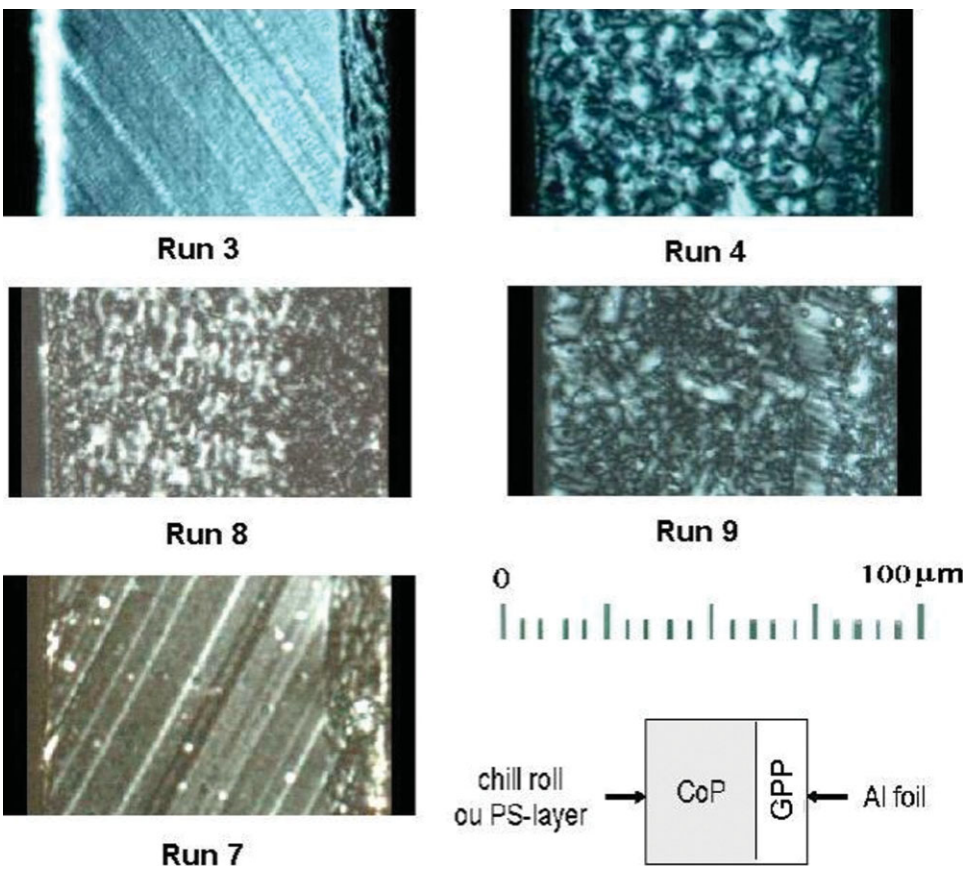


**Figure 14** Morphology in the thin sections of the polypropylene films observed by optical microscopy for various operating conditions. [Color figure can be viewed in the online issue, which is available at www.interscience.wiley.com.]

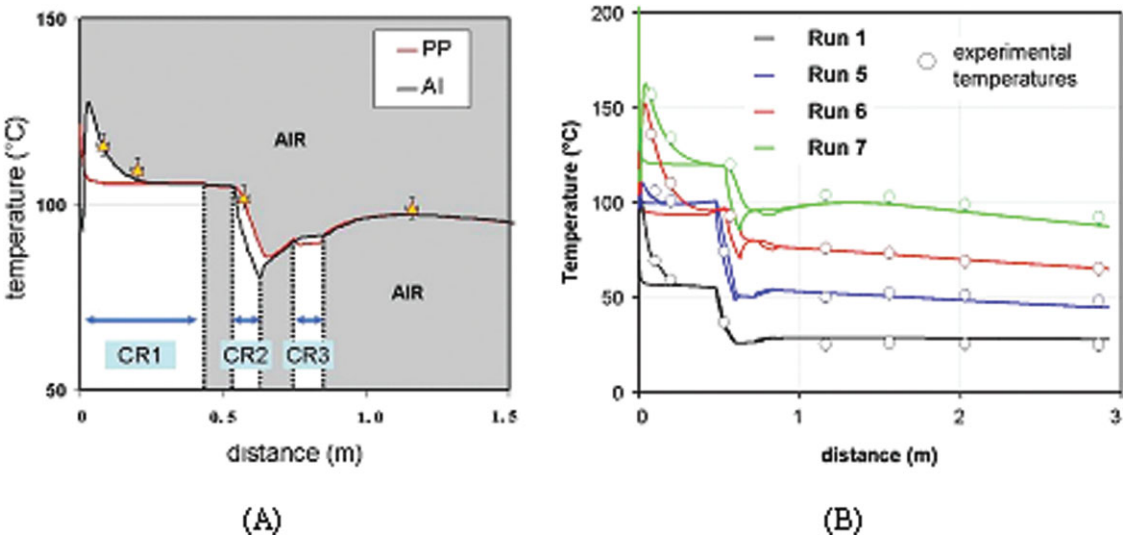


**Figure 15** A: Computed temperature field along the process for Run 6 and boundary conditions: $U_t = 0.67$ m/s and $T_{CR1} = 105°C$. B: Comparison between experimental and numerical temperature fields for several cooling conditions ($U_t = 0.42$ m/s). The two lines correspond to the upper (Al) and lower surface (PP) temperatures of the multilayered structure, respectively. [Color figure can be viewed in the online issue, which is available at www.interscience.wiley.com.]

polypropylene crystallized above 100°C, as demonstrated by the comparison between Figures 13(D) and 16(A). This is consistent with the literature which points out that crystallization temperature range of the β phase is 100–130°C.[21] On the other hand, the X-ray pattern of Figure 13(E) and the microscopy observation in Figure 14 show that polymer layers had not enough time to crystallize totally for Run 7. Few spherulites are observed within amorphous and smectic phases. Because of a high line speed, polypropylene cannot crystallize totally during cooling on the first chill roll. Then, polypropylene film was quenched onto the second regulated roll (CR2) whose temperature was below 25°C. This crystallization sequence is clearly explained by the curves of temperature and transformed fraction in Figure 16(B) and would not be understandable without the help of simulation. This quenching step explains the presence of smectic phase in the bulk. All these correlations confirm that our model can predict accurately not only the temperature history but also the crystallization of polymer layers.

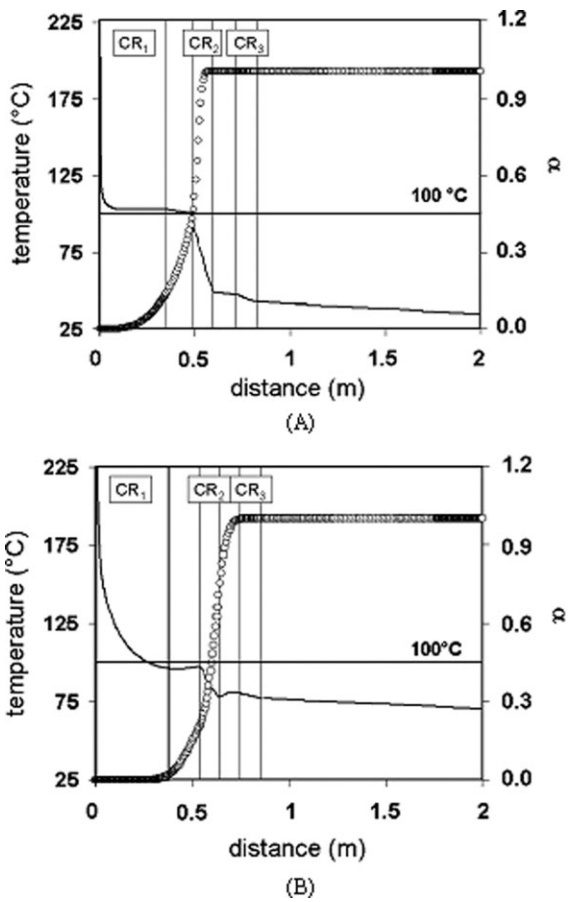


**Figure 16** Evolution of transformed volume fraction (○) and temperature (—) in the middle (≈ 30 μm) of the polypropylene layer (CoP): (A) Run 9: $U_t = 0.08$ m/s and $T_{CR1} = 103°C$, (B) Run 7: $U_t = 0.42$ m/s and $T_{CR1} = 94°C$.

### Mechanical properties of polymer films

The values of the peeling force are reported in Table I. They correspond to peel energy data which vary from 0 to 1500 J/m$^2$ according to the processing parameters. Absolutely no correlation could be established between these peel energy data and processing parameters.

The mechanical properties of the polymer films (Young's modulus and yield stress) were investigated for several process conditions by DMA and

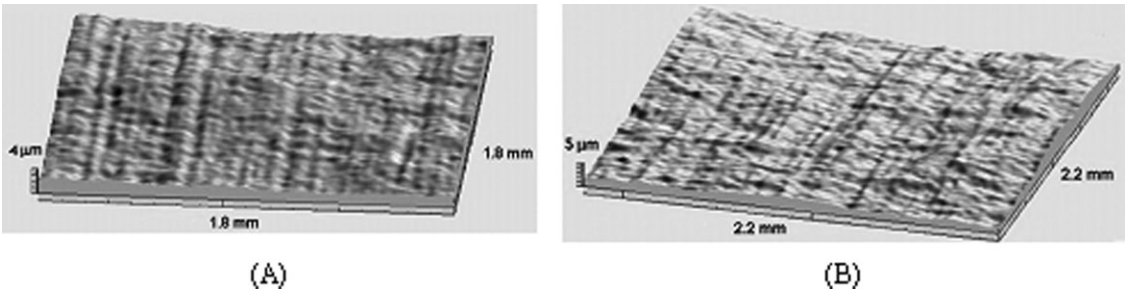


**Figure 17** 3D-microtopography of surface roughness at the interface: (A) aluminum foil and (B) grafted polypropylene layer.

tensile tests. As shown in Table II, both yield stress and Young's modulus are maximum when the polymer film has crystallized at high temperature (Runs 4, 6, and 9). The smallest values are measured when the polymer film contains smectic phase (Runs 3, 5, and 7). By correlating yield stress and Young's modulus with morphology observations, we notice that both increase with the degree of crystallinity, as already described in literature.[23–26]

## Discussion of adhesion mechanisms

### Mechanical anchoring

In some cases, adhesion can be promoted by mechanical anchoring, especially if the coated surface is porous. Stralin and Hjertberg[27] have tested the ability of various low density polyethylenes with different melt indices to penetrate the pores of aluminum oxides. By examining the roughness of the polymer film and the aluminum surface by scanning electron microscopy (SEM), they suggested that high adhesion values could be attributed to a better mechanical anchoring into the pores.

To test this hypothesis, we characterized the wetting of the aluminum surface by the polymer film after extrusion coating. The two antagonist surfaces were characterized by noncontact surface microtopography and AFM for two extreme process conditions (Runs 3 and 7) which correspond to poor and high adhesive strengths, respectively. Figure 17 shows the spatial reconstruction for Run 3 of the surface topography on a large scale ($2 \times 2$ mm$^2$). Rolling marks are clearly observed on the aluminum foil in Figure 17(A) and reproduced on the polymer surface as an inverted image in Figure 17(B). The average roughness $R_a$ is the same in both cases ($R_a = 0.1$–$0.2$ µm). Furthermore, AFM characterization at a smaller scale ($15 \times 15$ µm$^2$) leads to a close result visible in Figure 18(A,B). Marks can be also distinguished on the two surfaces but their depths are around 300 nm for the aluminum foil and 150 nm for the polymer film, respectively.

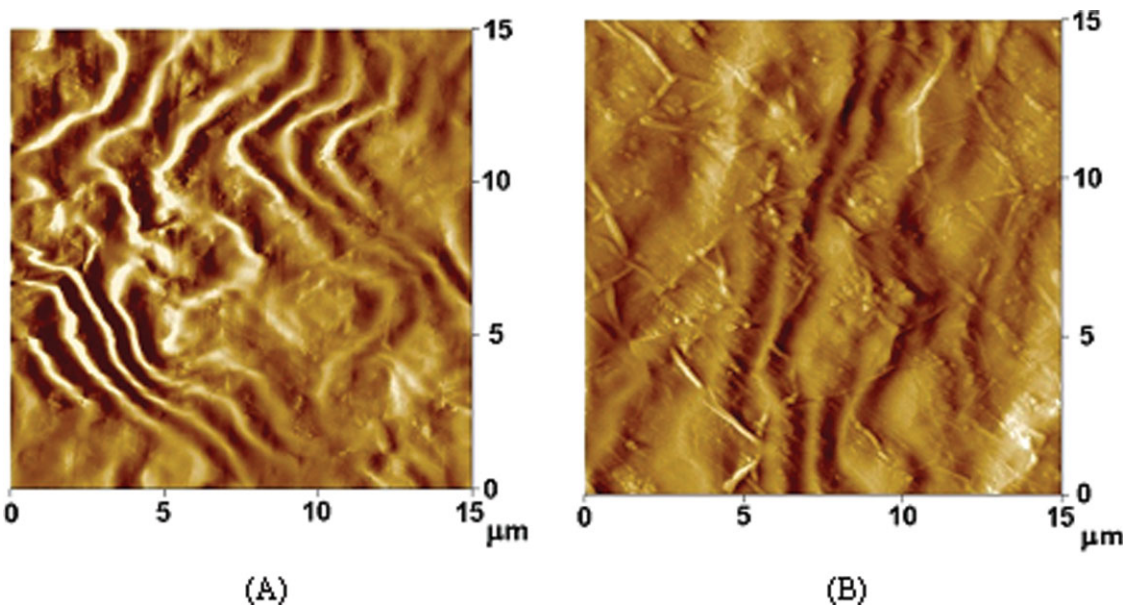


**Figure 18** Surface topography at the interface caught by AFM: (A) aluminum foil and (B) grafted polypropylene layer. [Color figure can be viewed in the online issue, which is available at www.interscience.wiley.com.]

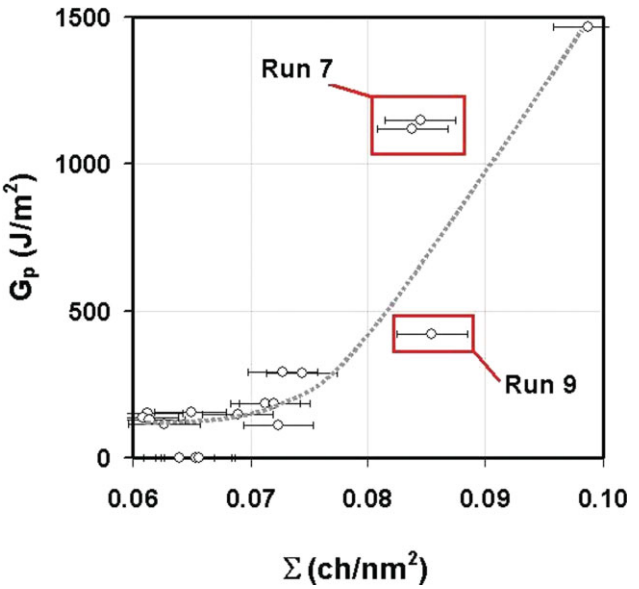


**Figure 19** Effect of the surface density of bonds on the peel energy $G_p$ for several process conditions. [Color figure can be viewed in the online issue, which is available at www.interscience.wiley.com.]

These results tend to show that molten polymer has enough time to wet large scale surface roughness of the aluminum foil during the nip step, but this is less clear for the small scale surface roughness as investigated by AFM. The small difference of the mark depths observed by AFM could be linked to a relaxation of the polymer film after dissolution of the aluminum foil or to a partial wetting of the aluminum surface. For Run 7, similar observations have been made both by surface topography and by AFM.

As a conclusion, the mechanical anchoring cannot explain the large differences between the measured adhesive strengths observed in Table I.

### Relationship between adhesion energy and density of bonds Σ

The bond densities determined according to our protocol are significantly different, which makes it possible to compare the multilayered structures for all the process conditions. Figure 19 clearly highlights that peel energy rises with the density of bonds created at the interface GPP/Al during the cooling step. It must be recalled that no direct correlation could be established between the peel energy and any processing parameter.

### Correlation between temperature history and density of bonds

The density of bonds created at the interface strongly depends on the cooling conditions. The chemical reaction is blocked or drastically lowered when the polymer crystallizes. Indeed, the reaction probability is mainly linked to molecular mobility at the interface which strongly decreases at low temperature or during crystallization. A parameter $\psi$ has been defined to quantify the impact of cooling conditions on density of bonds:

$$\psi = \int_0^{t_0} T(t)dt \tag{3}$$

where $T$ is the temperature calculated near the interface aluminum-GPP (distance to the interface = 2 μm) and $t$ the time elapsed from the die exit; $t_0$ is the time of the onset of crystallization (transformed volume fraction $\alpha = 0.01$).

To know the temperature history impact on the chemical reaction at the interface, we have plotted in Figure 20(A) the density of bonds as a function of the parameter $\psi$. It is interesting to note that the

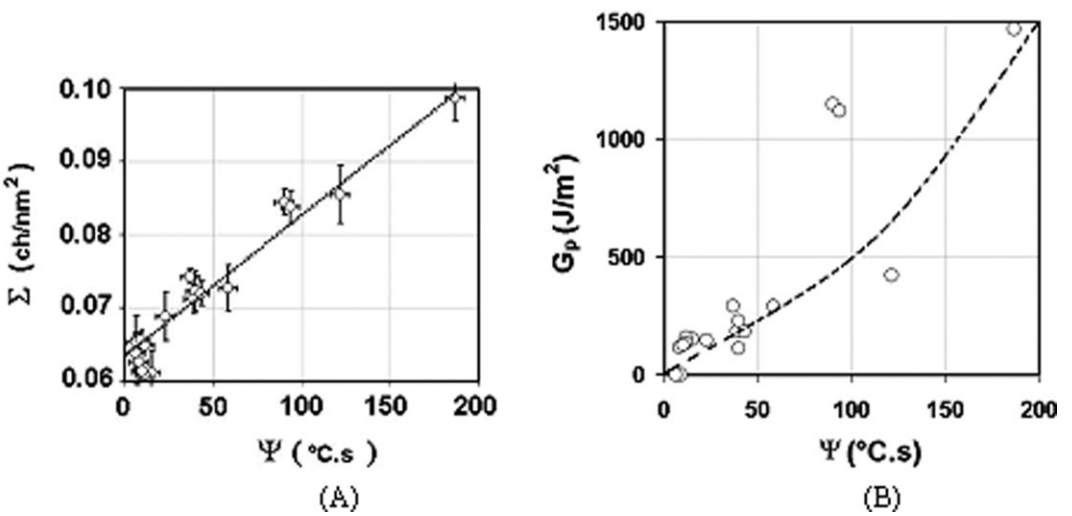


**Figure 20** (A) Effect of temperature history on the surface density of bonds Σ and (B) effect of temperature history on peel energy.

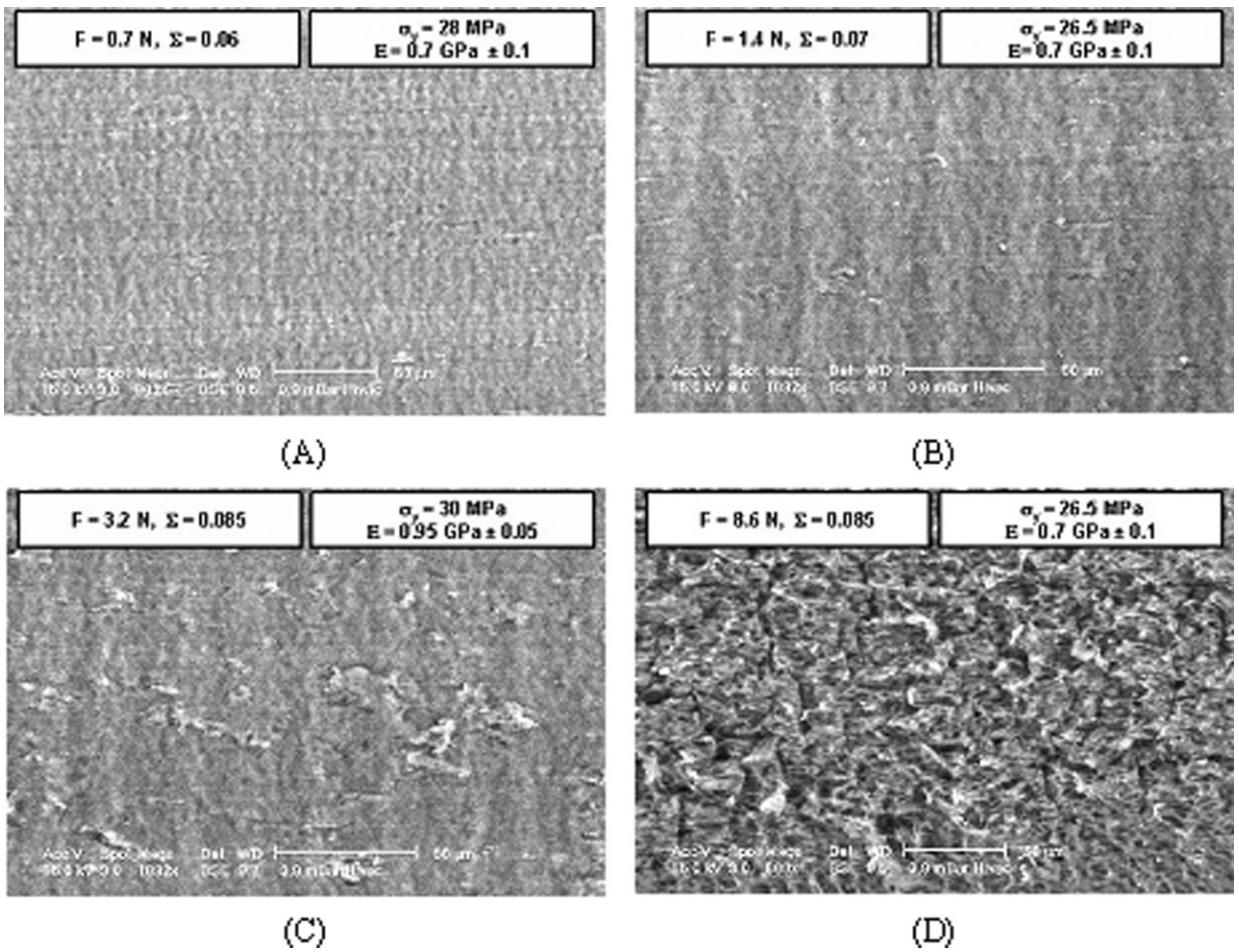


**Figure 21** Characterization of the polymer surface after the peel test by SEM for several cooling conditions: (A) Run 1: $U_t = 0.42$ m/s and $T_{CR1} = 56°C$, (B) Run 5: $U_t = 0.42$ m/s and $T_{CR1} = 100°C$, (C) Run 9: $U_t = 0.08$ m/s and $T_{CR1} = 103°C$, (D) Run 7: $U_t = 0.42$ m/s and $T_{CR1} = 94°C$.

number of chemical links increases when $\psi$ rises. Therefore, the chemical reaction seems to be very sensitive to high chill roll temperatures ($T_{CR1}$), high process velocities ($U_t$), or the presence of an additional layer (see Runs 5–7 and Runs 9–10), which delay the beginning of crystallization, and this is consistent with the fact that the reaction between grafted polymer chains and aluminum oxides is thermally activated.[6] High temperatures certainly enhance the kinetic coefficient of the reaction which varies according to an Arrhenius law and increase the open time of the reaction, since crystallization is delayed. Moreover, the probability that a grafted chain close to the interface can react with aluminum oxide is improved because high temperatures promote polymer chain mobility.

Although empirical, the $\psi$ parameter was found to be a convenient way to compare different temperature histories and then, evaluate their impact on the chemical reaction. The plots of $G_p$ versus $\Sigma$ in Figure 19 and of $\Sigma$ versus $\psi$ in Figure 20(A) allow us to plot $G_p$ versus $\psi$ in Figure 20(B), which gives a correlation between adhesion and processing. All these plot highlight that adhesion in multilayered structures is mainly due to the formation of bonds at the interface which is promoted by high temperatures.

These results also show that the values of the density of chemical bonds determined here can be considered as representative of the processing conditions, even though they are not "pure" ones. We are aware of the simplifications used and of the imperfections of the method, from a physicochemical point of view, and additional experiments involving for instance nuclear magnetic resonance (RMN) should be necessary. This was out of the scope of the present article, aiming only at giving a physical interpretation of adhesion, taking into account processing conditions.

### Impact of the film mechanical properties on peel energy measurement

Figure 19 also revealed that peel energy might be significantly different although the measured densities of bonds were equal, e.g., for Runs 7 and 9.

This difference can be attributed to the ability of the polymer film to dissipate energy during the peel test. The dissipating phenomena during the peel test are clearly linked to the mechanical properties of the film close to the interface and in the bulk, which depend on the crystallization conditions. For instance, yield stress and elastic properties were very low when the polymer films were quenched and crystallized on a cold roll ($T_{CR} = 25°C$), as shown in Table II.

To illustrate this effect, we characterized the film interface by SEM after a peel test for different peel strength values. Figure 21 presents scanning electron micrographs of the polymer interface after peeling. Depending on the peel strength value and on the density of bonds, the surface can be smooth or rough. The roughness of the surface is attributed to the plastic deformation of the polymer surface and the formation of voids. A close comparison between the different micrographs reveals that plastic deformation occurs when the density of bonds is sufficient (up to 0.08 ch/nm$^2$). In this case, the mechanical properties of the polymer film are of prime importance because dissipating phenomena take place at the interface and in the bulk. Then, it appears that the lower the yield stress, the greater the plastic deformation. This remark explains that peel energy value is greater for Run 7 sample corresponding to Figure 21(D), in which the smectic phase is present due to quenching, than for Run 9 sample represented by Figure 21(C), in which only a spherulitic structure is observed, whereas the bond density is equivalent. The same trend was observed by Heuschling et al.[13] in the case of adhesion between grafted polypropylene and aluminum, or by Evans and Packham[28] in the case of adhesion between polyethylene and aluminum. They attributed the influence of quenching on adhesion to changes in the polymer mechanical properties, which increased the energy consumed up to the failure during peel test.

These complementary observations show that adhesion results from a complex interplay between the number of chemical bonds created at the interface and the capacity of the polymer layer to dissipate energy by plastic deformation.

## CONCLUSIONS

This study points out the impact of bond formation on adhesion in multilayered structures made by extrusion coating. Cooling steps along the whole process play a key role on the adhesion mechanisms, especially by improving or altering the surface density of bonds created between the grafted polypropylene chains and aluminum oxides. It appears that adhesion properties are very sensitive to high temperatures close to the interface "grafted polypropylene/aluminum," which increase the reaction rate and the open time for reaction. This time is strongly linked to the crystallization of the polymer layers because crystallization tends to block the reaction by decreasing the molecular mobility. As a consequence, the probability that a grafted chain close to the interface reacts with aluminum oxide drastically declines. This interface temperature will depend on stretching conditions, speed line, roll temperatures, and thickness of the multilayered structure.

The different experiments carried out to understand adhesion in polypropylene/aluminum structure showed that the mechanical anchoring contribution to adhesion was negligible compared with the created bonds contribution and the dissipating phenomena during peel test. In several cases, peel energy peaked up for high density of bonds due to plastic deformation of film. These cases correspond to samples with "poor" mechanical properties for the polymer film (i.e., low yield stress values) due to the presence of smectic phase.

As a conclusion, the design of the extrusion coating line (position and number of cooling rolls along the line), the cooling parameters (temperature of the chill rolls, line speed), and the polymer properties (molecular mobility, crystallization rate, etc.) are the key points for an optimization of adhesion in polypropylene/aluminum structures made by extrusion coating.

## References


1. Darque-Ceretti, E.; Felder, E. In Adhésion et Adhérence, Collection Sciences et Techniques de l'Ingénieur; CNRS Editions: Paris, 2003; p 313.
2. Wu, S. In Polymer Interface and Adhesion; Marcel Dekker: New York, 1982; p 279.
3. Cri, S.; Posser, H. J.; Wilson, A. D. J Mater Sci 1976, 11, 36.
4. Comien, P. Ph.D. Thesis, Université de Haute Alsace: France, 1987.
5. Hu, H.; Saniger, J.; Garcia-Alejandre, J. Mater Lett 1991, 12, 281.
6. Thery, S.; Jacquet, D.; Mantel, M. J Adhesion 1996, 56, 1.
7. Bistac, S.; Vallat, M. F.; Schultz, J. Appl Spectrosc 1997, 51, 1823.
8. Schneider, B.; Hennemann, O. D. J Adhesion 2002, 78, 779.
9. Schultz, J.; Lavielle, L.; Carre, A.; Comien P. J Mater Sci 1989, 24, 4363.
10. Pusset, P. Ph.D. Thesis, Université de Haute Alsace: France, 1994.
11. Kumpinsky, E. Ind Eng Chem Res 1993, 32, 2866.
12. Trouilhet, Y.; Morris, B. A. In Polymers, Laminations and Coatings Conference, Tappi Proceedings, 1999; p 457.
13. Heuschling, O.; Vanghluwe, P.; Reginster, L. J Adhes Sci Technol 1994, 8, 53.
14. Devisme, S.; Haudin, J. M.; Agassant, J. F.; Rauline D.; Chopinez, F. Intern Polym Process 2007, 22, 90.
15. Boucher, E.; Folkers, J. P.; Hervet, H.; Léger, L. Macromolecules 1996, 29, 774.
16. van den Brand, J. Ph.D. Thesis, Delft University of Technology: The Netherlands, 2004.
17. Davis, G. D. Surf Interf Anal 1993, 20, 368.

18. Olsson-Jacques, C. L.; Wilson, A. R.; Rider, A. N.; Arnott, D. R. Surf Interf Anal 1996, 24, 569.
19. van den Brand, J.; van Gils, S.; Beentjes, P. C. J., Terryn, H., de Wit, J. H. W. Appl Surf Sci 2004, 235, 465.
20. Weidinger, A.; Hermans, P. H. Makromol Chem 1961, 50, 98.
21. Cheng, S. Z. D.; Janimak, J. J. J.; Rodriguez, J. In Polypropylene. Structure, Blends and Composites, Vol 1; Karger-Kocsis, J., Ed.; Chapman & Hall: London, 1995; p 31.
22. Cotto, D.; Duffo, P.; Haudin, J. M. Intern Polym Process 1989, 4, 103.
23. Akay, M.; Barkley, D. Plastics Rubber Process Applicat 1984, 4, 247.
24. Akay, M. Brit Polym J 1989, 21, 285.
25. Rettenberger, S.; Capt, L.; Münsted, H. Rheol Acta 2002, 41, 332.
26. Rolando, R. J.; Krueger, D. L.; Morris, H. W. ACS Polym Mater Sci Eng 1985, 52, 76.
27. Stralin, A.; Hjertberg, T. J Adhes Sci Technol 1993, 7, 1211.
28. Evans, J. R. G.; Packham, D. E. Int J Adhesion Adhesives 1981, 1, 149.